The Influence of Mock Circulation Input Impedance on Valve Acceleration During *In Vitro* Cardiac Device Testing

M. Keith Sharp,* Christopher M. Richards,* Kevin J. Gillars,† Guruprasad Giridharan,† and George M. Pantalos†

For a mechanical heart valve, a strong spike in pressure during closing is associated with valve wear and erythrocyte damage; thus, for valid *in vitro* testing, the mock circulation system should replicate the conditions, including pressure spikes, expected *in vivo*. To address this issue, a study was performed to investigate how mock circulation input impedance affects valve closure dynamics. A left ventricular model with polyurethane trileaflet inflow valve and tilting disc outflow valve was connected to a Louisville mock circulation system, which incorporates 2 adjustable flow resistors and 2 compliances. In the study, 116 cases matched zero frequency modulus well (982–1147 dyn · s/cm^5), but higher harmonics were purposely varied. Acceleration measured at the outflow valve ring (42.4–89.4 milli-Gs) was uncorrelated with impedance error (74.1–237 dyn · s/cm^5 relative to target impedance), but was correlated with end-systolic impedance (1082–1319 dyn · s/cm^5) for cases with high zero frequency modulus, which exhibited just less than full ejection. These differences demonstrate that mock circulation response affects the magnitude of the closing spike, indicating that control of this parameter is necessary for authentic testing of valves. Correlation of acceleration to end-systolic impedance was weak for low zero frequency modulus, which tended toward full or hyperejection, reinforcing common laboratory observations that valve closing also depends on ventricular operating conditions. *ASAIO Journal* 2008; 54:341–346.

Important criteria of cardiac device performance are the associated levels of hemolysis and thrombogenesis, which can be influenced by time dependent flow patterns within the device. Device reliability can also be affected by the flow waveform. As an important example, prosthetic valve wear and hemolysis have been attributed to high temporal pressure gradients, which produce strong flow accelerations and distinctive spikes in aortic pressure waveforms during valve closure. In contrast to animal model results, it was found in early human trials of artificial hearts that the systolic fraction of the heart beat cycle could be increased, thereby decreasing the maximum temporal pressure gradient and reducing blood damage.[1–4] The objective of this project was to identify characteristics of the dynamic response of an *in vitro* load that should be controlled to mimic physiologic operating conditions and ensure valid performance and reliability testing of prosthetic valves. The quantitative indicator of dynamic response utilized was input impedance, which is the frequency-dependent ratio of pressure and flow rate. The measured parameter related to valve performance and reliability was acceleration at the valve ring, which is closely coupled to the impact of valve closing. Therefore, the specific hypothesis of this study was that load input impedance affects valve ring acceleration.

From the *Department of Mechanical Engineering, and †Cardiovascular Innovation Institute, University of Louisville, Louisville, Kentucky.

Submitted for consideration February 4, 2008; accepted for publication in revised form April 14, 2008.

Reprint Requests: M. Keith Sharp, Department of Mechanical Engineering, 200 Sacket Hall, University of Louisville, Loiusville, KY 40292. Email: keith.sharp@louisville.edu.

DOI: 10.1097/MAT.0b013e31817c6aeb

Materials and Methods

Experimental Design

An adult mock circulation system was used to determine the effect of vascular input impedance on the dynamics of valve closure for a rigid tilting disc outflow valve. The ventricular sac driveline pressure (180 mm Hg), heart rate (66 bpm), and systolic fraction (30%) were set at the pneumatic heart driver, then vascular resistance and compliance were adjusted initially to produce clinically normal values of mean arterial pressure (75–110 mm Hg), cardiac output (~5.8 lpm), and left ventricular end diastolic pressure (~12 mm Hg).[5] Atrial pressure was maintained in a physiologic range (~12 mm Hg) throughout the experiments by adjusting the fluid volume in the system. After the initial tuning to produce the normal baseline condition, the ventricular sac drive line pressure, systolic fraction, and heart rate were not altered.

Valve dynamics were characterized by acceleration at the valve ring for 116 cases over a range of vascular input impedance. For each case, mock circulation system elements were adjusted manually and the root mean squared error (RMSE) of measured impedance relative to the target impedance[6] was calculated for the first 4 harmonics. For baseline cases, RMSE was minimized. For the other cases, distal resistance was adjusted to retain a good fit of the zeroth harmonic, whereas proximal resistance, proximal compliance, and inertance were purposely misadjusted to increase RMSE. Distal compliance was constant. Two proximal resistance configurations included the baseline value and a reduced value produced by removing the filter material from its chamber in the mock circulation system. Four proximal compliance configurations included the baseline spring and a lighter spring and the addition of 300 ml of air to the compliance chamber with each spring. Four inertance configurations included the baseline length of 25 mm diameter Tygon tubing at the entrance of the mock circulation system plus longer lengths equal to 125%, 150%, and 200% of baseline. All cases, therefore, had nearly

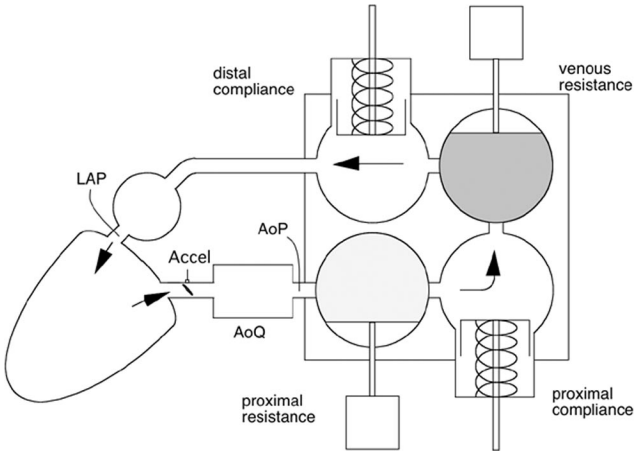

Figure 1. Mock circulation and instrumentation schematic. Measured parameters were left atrial pressure (LAP), valve ring acceleration (Accel), aortic flow (AoQ), and aortic pressure (AoP).

identical mean flow and pressure, but differed in higher order response.

Mock Circulation

The adult mock circulation consisted of atrium, ventricle, and systemic and coronary vasculature components as illustrated in (**Figure 1**). In a previous study, the adult mock circulation was shown to mimic human normal ventricle, failing ventricle, and partial cardiac recovery physiological responses as defined by characterizing hemodynamic parameters, ventricular pressure-volume relationship, aortic input impedance, and vascular mechanical properties.[7] An artificial atrium,[8] made of a flexible polymer sphere 50 mm in diameter, was connected upstream of the inflow valve of a mock ventricle, which consisted of a flexing, polymer sac inside a pressurization chamber.[9] The ventricular sac was hemi-ellipsoid shaped, 70-mm wide at the base, and 83-mm long from base to apex. The base was covered by a semirigid polymer dome 20-mm high, with mounts for inflow (mitral) and outflow (aortic) prosthetic valves. The ventricular model[10] was fitted with a flexible polyurethane trileaflet inflow valve and a rigid tilting disc outflow valve (Medtronic Hall 25 mm, Medtronic, Inc., Minneapolis, MN), so that the predominant feature of the acceleration signal would be the outflow valve closing spike.[11] The downstream valve ring incorporated a short cylindrical section and a barb for connecting 25 mm Tygon tubing. Metered pulses of compressed air (Utah Drive, SynCardia Systems, Tucson, AZ) were delivered to the pressurization chamber during systole, compressing the ventricular sac to form coapting quadrants simulating contraction of the ventricle and the delivery of cardiac stroke volume. A short 2.0-cm long section of 25-mm diameter Tygon tubing connected the outflow valve of the ventricular sac to the mock systemic vasculature. The length of tubing influences the impedance measured by the sensors, primarily by adding inertance to the system. Therefore, the length was minimized to best match the target impedance. The Louisville mock vascular system (which comprises a modification of the Utah system[12,13]) used in this study consists of a polycarbonate block into which cylindrical cavities were machined for compliances and resistances. The systemic unit consists of a proximal (characteristic aortic) resistor, proximal compliance, distal (peripheral) resistor, and distal compliance. The system uses open-cell foam or a folded fiber sheet for proximal resistance that was adjustable by compressing the material with a motorized piston and a distal resistance made of porous plastic adjustable by occluding the plastic with a flexible rubber bulb. Proximal and distal compliance elements were formed by coil spring-loaded bellows adapted from the Penn State mock circulation[8] by Woodruff *et al.*[14]

Instrumentation

Valve ring longitudinal acceleration was measured with a PCB precision quartz shear ICP accelerometer (PCB 353B16, 9.46 mV/G sensitivity, 1 Hz to 10 kHz range, ±500 G peak amplitude) glued to the cylindrical section of the valve ring. The accelerometer was oriented to measure positive acceleration in the direction of flow out of the left ventricle during systole. A clamp-on ultrasonic flow sensor (model H20XL, Transonic Systems, Ithaca, NY) was placed immediately downstream of the barb on the valve ring housing to measure aortic flow. A high fidelity pressure catheter (Mikro-tip catheter transducer model MPC-500, Millar Instruments, Houston, TX) was inserted through an introduction port downstream of the flow sensor to measure aortic pressure. A second pressure catheter (also Millar MPC-500) was inserted between the atrium and the inflow valve to measure atrial pressure.

Acceleration signals were conditioned by a National Instruments SCXI-1530 signal conditioning module (National Instruments, Austin, TX) with an antialiasing filter set at 2,500 Hz. Data were digitally recorded by a data acquisition card (National Instruments PCI-6052E) at a 5,000 Hz sampling rate. Pressure and flow transducers were pre- and postcalibrated, and transducer gains and offsets calculated and applied to ensure measurement accuracy. Signal conditioning was accomplished using pressure transducer amplifiers (Ectron, San Diego, CA), a transit-time flow meter (model T110, Transonic Systems, Inc.), and other peripheral conditioners integrated in an instrumentation system compliant with Good Laboratory Practice (GLP) guidelines.[15] Signal conditioned hemodynamic data were low-pass filtered at 60 Hz, analog-to-digitally converted (AT-MIO-16E-10 and LabVIEW, National Instruments) at a sampling rate of 400 Hz, and stored on a separate personal computer for postprocessing and analysis.[16]

Data Analysis

Hemodynamic parameters and vascular input impedance were calculated using the Hemodynamic Evaluation and Assessment Research Tool (HEART) program[17] and supporting m-files developed in Matlab (MathWorks, Natick, MA). All hemodynamic parameters were calculated on a beat-to-beat basis and averaged over the entire data set to obtain a mean value for each parameter.

Input impedance for the mock vasculature was derived from aortic pressure (AoP) and flow (AoQ) waveform measurements recorded during each test condition. Using 30-second data epochs, the waveforms were converted from time to frequency domain using Fast Fourier Transform (FFT) algorithms in Matlab. The magnitudes and phases of input impedance were calculated as the ratio of the magnitudes of distal aortic pres-

sure and flow at each harmonic, and the difference between the phases at each harmonic, respectively. An uncertainty analysis was also performed to estimate the error in the input impedance terms resulting from experimental error.

In addition to mock circulation input impedance as a function of frequency, impedance magnitudes at the end of systole were calculated. Because hydraulic power and signal-to-noise ratio diminish with increasing frequency, and the uncertainty error in impedance increases with increasing harmonics, only the zeroth and first 3 harmonics were included in RMSE and in end-systolic impedance. In preliminary experiments, it was confirmed that the hydraulic power of the fourth and higher harmonics was less than about one percent of the zeroth. Mean autopower spectra of the acceleration signals were calculated by averaging the autopower spectra of individual accelerations for each cardiac cycle.

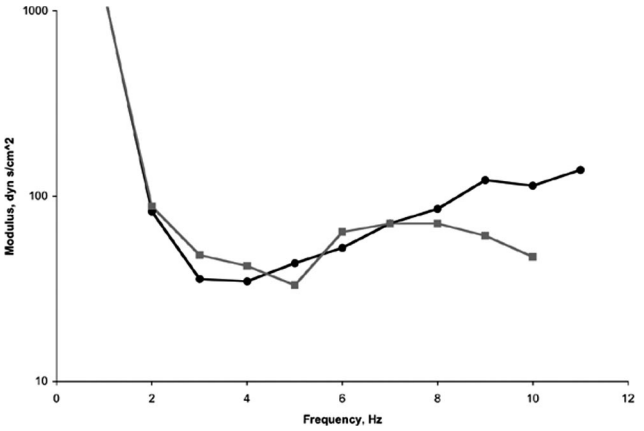

Figure 3. Input impedance of example low resistance and high compliance case (round symbols) compared with the target (square symbols).

Results

Modulus and phase of input impedance of 3 example cases are compared with the target impedance in **Figures 2** through **4**. For the baseline (minimum RMSE) setting (**Figure 2**), the first harmonic modulus is very close to the target, while the phase is slightly high. For the second harmonic, the modulus is slightly low, and the phase is high but still negative. For the third harmonic, the modulus is slightly low, and the phase is positive and significantly larger than the target, which is slightly negative. The zero frequency crossover is at a significantly lower frequency than the target.

For the second example case (**Figure 3**), which represents a low resistance and high compliance setting, the modulus falls more gradually and phase is more negative over the low frequency range. RMSE is roughly twice that of the baseline case. For the first harmonic, the modulus is high, whereas the phase is closely matched to the target. The second harmonic modulus remains high, whereas the phase is low. For the third harmonic, the modulus and phase are slightly low. The zero frequency crossover matches well.

For the third example case (**Figure 4**), which represents a high inertance and high resistance setting, the modulus is low for the first harmonic, high for the second harmonic, and very high for the third harmonic, whereas the phase is high for the first harmonic and very high for the second and third harmonics. The zero frequency crossover is between the first and second harmonics, whereas for the target, it is above the third harmonic. RMSE is roughly 3 times that of the baseline case.

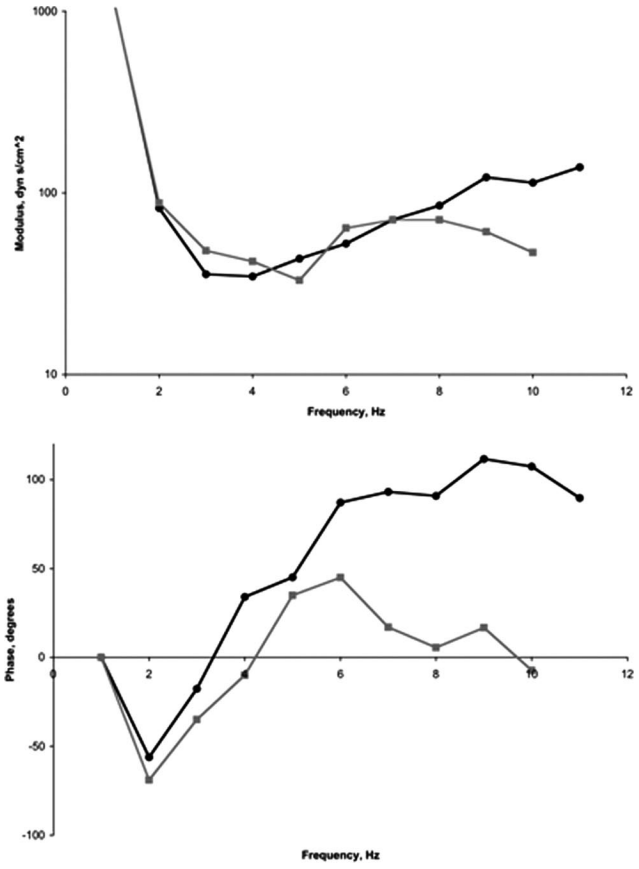

Figure 2. Input impedance of example baseline case (low RMS error case, round symbols) compared with the target (square symbols).

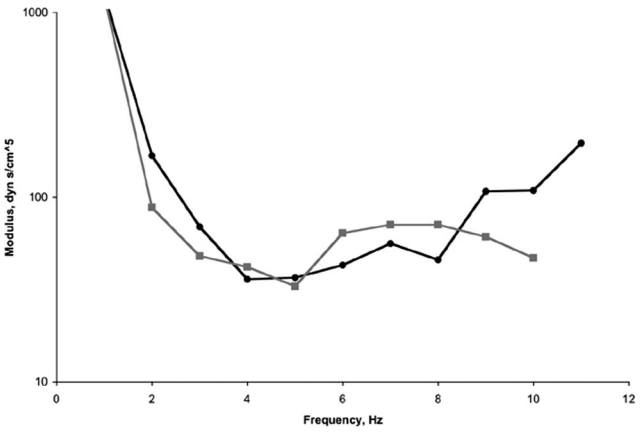

Figure 4. Input impedance of example high inertance and high resistance case (round symbols) compared with the target (square symbols).

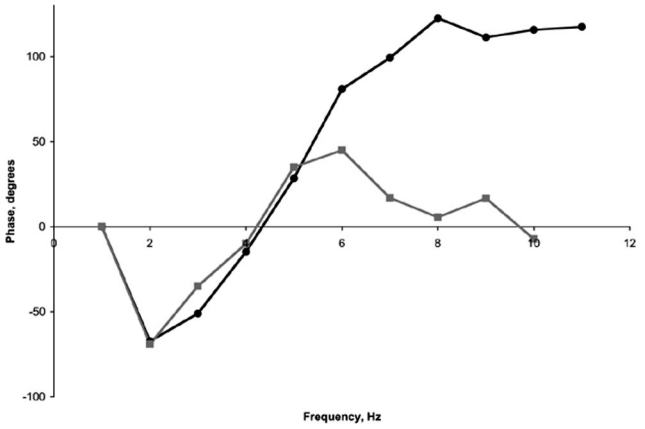

Figure 5. Typical valve acceleration response time history.

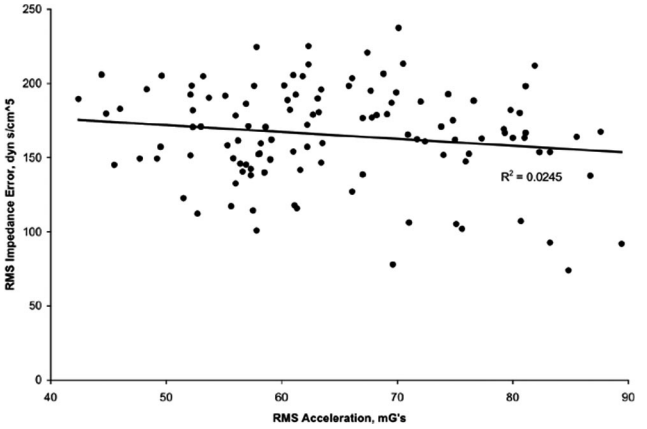

Figure 7. Dependence of RMS acceleration on RMS impedance error. Sloped line is linear fit of all cases.

A sample acceleration time history measured at the valve ring is illustrated in (**Figure 5**). The accelerometer measured positive acceleration in the direction of flow out of the left ventricle during systole. Consequently, peak acceleration is negative since closure of the aortic valve induces a force on the valve ring in the direction of regurgitant flow during diastole. The positive "rebounding" acceleration response immediately after peak acceleration is a result of compliance and rigid body response of the system. Impact force from the valve occluder onto the valve ring creates a broad spectrum excitation and corresponding acceleration response as seen by the autopower spectrum of the acceleration signal in (**Figure 6**). Results were similar for all mock circulation configurations with the exception of varying amplitudes. The peak at 2,100 Hz is likely due to a structural mode of vibration of the mock circulation system.

For the 116 cases, mean aortic pressure varied from 64.5 to 72.6 mm Hg with an average of 68.8 and standard error of 0.17 mm Hg, whereas mean flow rate varied from 4.82 to 5.55 L/min with average 5.21 ± 0.01 L/min. RMS error between actual and target impedance of the zeroth and first 3 harmonics ranged from 49.3 to 237 dyn · s/cm^5 with average of 160.7 ± 3.59 dyn · s/cm^5 whereas the zero frequency modulus varied from 982 to 1147 dyn · s/cm^5 with average of 1057 ± 3.13 dyn · s/cm^5 The instantaneous impedance at the end of systole, calculated for the zeroth and first 3 harmonics, varied from 1071 to 1319 dyn · s/cm^5 with average of 1179 ± 5.03 dyn · s/cm^5 RMS accelerations measured at the valve ring ranged from 42.4 to 89.4 milli-G's (mG's) with average of 64.5 ± 1.03 mG's. Acceleration did not correlate well with RMS error of impedance (**Figure 7**), nor with zero frequency impedance (**Figure 8**). Acceleration for all 116 cases was only weakly correlated with end-systolic impedance (**Figure 9**). However, when the cases are divided into 2 groups above and below end-systolic impedance of 1064 dyn · s/cm^5, good correlation was obtained for high end-systolic impedance (**Figure 10**). In **Figures 7–9**, all individual data points are shown. In **Figure 10**, results for repeated experimental conditions are averaged, which decreased scatter by a small amount.

The pressure waveforms were evaluated for all 116 cases for indications of full or hyperinflation. Only a few cases of hyperinflation were found, identified by dual peaks in pressure during systole before valve closing. Full inflation was identified by a distinct shoulder in the rising pressure during systole. Of the 116 cases, 40 were partial ejection and 76 were full or hyper ejection. These 2 groups were compared with ANOVA methods. Although the ranges of end-systolic impedance for the 2 groups overlapped, the means (1065 dyn · s/cm^5 for

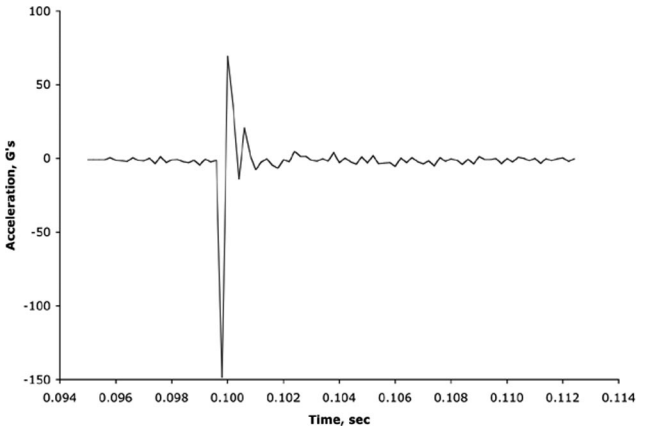

Figure 6. Typical valve acceleration autopower spectra.

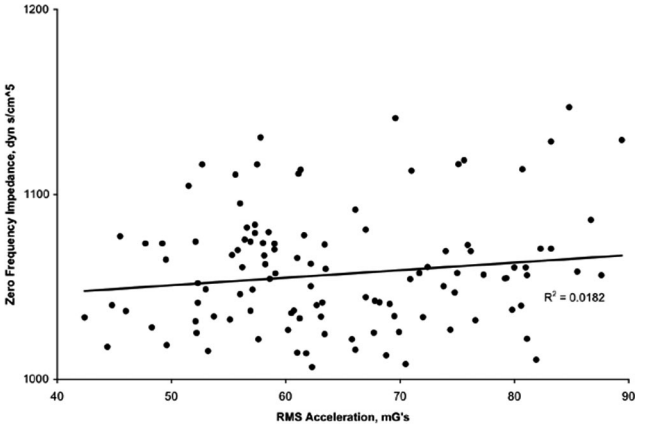

Figure 8. Dependence of RMS acceleration on zero frequency impedance. Sloped line is linear fit of all cases.

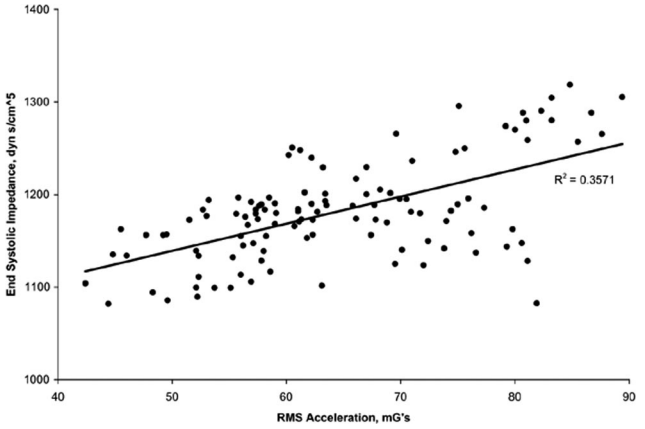

Figure 9. Dependence of RMS acceleration on end-systolic impedance. Sloped line is linear fit of all cases.

partial ejection and 1053 dyn · s/cm^5 for full/hyperejection) were different with a confidence level of $p = 0.069$.

Discussion

This study focused on the potential influence of mock circulation response on outlet valve dynamics. The spectrum of the acceleration of the valve ring after valve impact at the end of systole depends on the mechanical response of the valve, artificial heart, mock circulation and all other attached structures, as well as the dynamics of the enclosed fluid. These variables were held constant, except for changes associated with adjustments to mock circulation impedance. Preliminary tests assured that these changes did not significantly impact the acceleration spectrum. The magnitude of acceleration, however, is strongly influenced by the hydraulic response of the system (**Figure 10**), specifically, the fluid forces acting on the valve during its closing motion. Impedance magnitudes at the end of systole provide a useful indicator of the influence of mock circulation response on valve closure. Since high impedance is normally associated with high pressure, increased end-systolic impedance would be expected to produce higher acceleration, which is confirmed in **Figure 10** for the high zero frequency impedance group.

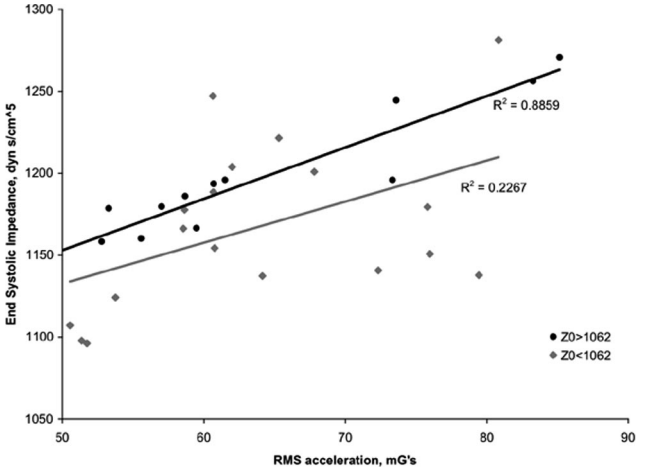

Figure 10. Dependence of RMS acceleration on end-systolic impedance. Upper sloped line is linear fit for zero frequency impedance >1,062 dyn · s/cm^5 lower line is for zero frequency impedance <1,062 dyn · s/cm.^{5}

Valve acceleration did not correlate with root-squared error of input impedance (**Figure 7**). A finite mismatch of impedance may cause higher or lower acceleration than the target. Furthermore, since impedance is the ratio of pressure and flow, even a perfect impedance match does not necessarily constrain the valve closing pressure to a target value. However, if pressure and flow waveforms are reasonably physiologic, a close impedance match would tend to ensure a close match with target valve acceleration.

Similarly, valve acceleration did not correlate with zero frequency impedance (**Figure 8**). This result should serve as a warning to device testers that controlling mean pressure and flow is insufficient for producing a truly physiologic device response. Additional factors related to dynamic system response and device operating conditions must be considered to avoid exposing valves to closure conditions that under or over represent those that prevail *in-vivo*.

The system response in this study influences the low frequency external excitations causing the motion of the valve. However, as a result of short duration impacts of the valve leaflet with the valve ring, measured acceleration response of the valve (**Figure 5**) contains high frequency content as revealed in the valve acceleration spectrum (**Figure 6**). The amplitude of this spectrum is a result of both the low frequency external hydraulic excitation and the structural dynamics of the system. When comparing valve acceleration among different mock circulation systems, it may be necessary to consider not only the valve acceleration time history and corresponding spectrum, but also the differences in structural dynamic characteristics among the systems.

Device operating conditions, specifically ventricular ejection, seems to have influenced the results. High zero frequency impedance tends to reduce flow, limit ejection, and produce consistent valve motion. In these experiments, however, varied dynamic response of the mock circulation system clouded this relationship, *i.e.*, while well-correlated cases with zero frequency impedance above 1064 (**Figure 10**) were more likely to be partial ejection, the division between the groups was not absolute. Nonetheless, the small *p*-value ($p = 0.069$) comparing zero frequency impedance between the ejection condition groups, whereas not lower than the usual $p = 0.05$ threshold for statistical significance, is sufficiently small to suggest that the more consistent partial ejection condition allowed the influence of end-systolic impedance on valve acceleration to appear. On the other hand, the greater tendency for full and hyperejection within the low zero frequency impedance group caused inconsistency in valve closing excitations and, therefore, scatter in valve acceleration values.

The difference between the largest and smallest valve acceleration values is over 100%. For components susceptible to fatigue failure, including valve occluders and many other critical parts in artificial hearts, such a change in stress level may significantly impact the time-to-failure of the component. Even a small error in modeled stress in *in vitro* reliability testing relative to *in vivo* operating conditions may cause a large inaccuracy in measured cycle life if the stresses are near the endurance limit of the material or if the slope of the stress versus cycle life curve is shallow.

Conclusion

This study shows that the oscillatory components of hydraulic load impedance can have an influence on outflow valve acceleration during closing. Further, results indicate that simply matching a target impedance spectrum within a given tolerance may be insufficient for modeling physiologic response. Rather, the details of dynamic response may be important, *e.g.*, in the case of outflow valve closure, end-systolic impedance was shown to provide an indicator of the excitation force for valve impact on its seat. Impedance values at other times may be important for other cardiovascular device components. For instance, for the pneumatic artificial heart diaphragms, end diastolic impedance may influence diaphragm tension and, therefore, diaphragm life. Similar dependence on load impedance might be expected for a wider range of components of cardiovascular devices, including artificial hearts and ventricular assist devices, for which the motion and dynamic behavior of components are coupled to the response of the load.

While load impedance is directly related to bulk flow and pressure exerted on the device and thereby influences component motion, local flow and pressure fields determine the spatial and temporal distribution of flow-induced stresses on component surfaces and, thus, may modify the details of the impedance/component motion relationship. Measurements of these local parameters were not available in these studies, thus one can only speculate about their potential importance in this case. Load impedance is, therefore, one among a number of parameters that may need to be controlled to ensure kinematic similitude for authentic performance and reliability testing of devices.

Acknowledgment

The authors thank the Jewish Hospital Research Foundation and the Cardiovascular Innovation Institute for use of facilities and SynCardia Systems for use of the heart driver.

References

1. Ross J Jr: Framework for analysis of ventricular function and overall circulatory performance, in West JB (ed), *Best and Taylor's Physiological Bases of Medical Practice,* 11th ed. Baltimore, MD, Williams & Wilkins, 1985, pp. 284–295.
2. Levinson MM, Copeland JG, Smith RG, *et al*: Indexes of hemolysis in human recipients of the Jarvik-7 total artificial heart: A cooperative report of 15 patients. *J Heart Transplant* 3: 236–248, 1986.
3. Stelzer GT, Ward RA, Welhausen SR, *et al*: Alterations in select immunologic parameters following total artificial heart implantation. *Artif Organs* 2: 52–62, 1987.
4. Mayes JB, Williams MA, Barker LE, *et al*: Clinical management of total artificial heart drive systems. *JAMA* 259: 881–885, 1988.
5. Shepherd JT, Vanhoutte PM: *The Human Cardiovascular System: Facts and Concepts.* New York, Raven Press, 1979, p. 325 (Appendix).
6. Nichols WW, Conti CR, Walker WW, Milnor WR: Input impedance of the systemic circulation in man. *Circ Res* 40: 451–458, 1977.
7. Pantalos GM, Gillars KJ, Ewert DL, *et al*: Characterization of an adult mock circulation for testing cardiac support devices. *ASAIO J* 50: 37–46, 2004.
8. Rosenberg G, Phillips WM, Landis DL, Pierce WS: Design and evaluation of the Pennsylvania State University mock circulation system. *ASAIO J* 4: 41–49, 1981.
9. Pantalos GM, Hayes J, Khanwilkar P, *et al*: Left ventricular simulator for cardiovascular device testing. *ASAIO J* 42: 46, 1996.
10. Pantalos GM, Chiang BY, Bishop DN, *et al*: Development of smaller artificial ventricles and valves made by vacuum forming. *Int J Artif Organs* 11: 373–380, 1988.
11. Pantalos GM, Kim CH, Flatau A: Variation in artificial heart acceleration and sound production with prosthetic valve selection in vitro. *Int J Artif Organs* 19: 181–188, 1996.
12. Sharp MK, Dharmalingam RK: Development of a hydraulic model of the human systemic circulation. *ASAIO J* 45: 535–540, 1999.
13. Gillars KJ: Design of a cardiovascular system hydraulic model. MS thesis. Department of Civil and Environmental Engineering, University of Utah, 2003.
14. Woodruff SJ, Sharp MK, Pantalos GM: Compact compliance chamber design for the study of cardiac performance in microgravity. *ASAIO J* 43: 316–320, 1997.
15. Koenig SC, Woolard C, Drew G, *et al*: Integrated data acquisition system for medical device testing and physiology research in compliance with good laboratory practices. *Biomed Instrum Technol* 38: 229–240, 2004.
16. Drew GA, Koenig SC: Biomedical patient monitoring, data acquisition, and playback with LabVIEW, in *Labview for Automative, Telecommunications, Semiconductor, Biomedical, and other Applications.* Upper Saddle River, NJ, Prentice Hall PTR, Chapter 2, 2000, pp. 92–98.
17. Schroeder MJ, Perrrault B, Ewert DL, Koenig SC: HEART: An automated beat-to-beat cardiovascular analysis package using Matlabä. *Comput Biol Med* 34: 371–388, 2004.